Open-Cell Flexible Polyurethane Foams: Comparison of Static and Dynamic Compression Properties

R. W. SHUTTLEWORTH, V. O. SHESTOPAL, and P. C. GOSS, *National Materials Handling Bureau, North Ryde, NSW 2113, Australia*

Synopsis

Dynamic stress–strain diagrams of polyurethane packaging foams have been obtained from free fall drop tests. The dynamic curves become higher as the deformation rates increase. An equation is proposed to describe the stress–strain dependence for different deformation rates. The model of filament buckling explains the form of the observed stress–strain dependence and phenomena related to repeated loading of the foam.

INTRODUCTION

Cushioning properties of plastic foams are usually estimated from one parameter only—the maximum deceleration of a product protected by cushioning. The insufficiency of such an approach is widely understood. Recently in Refs. 1 and 2 two more parameters have been proposed: ideality and efficiency of a cushioning material. However, all these parameters are strongly dependent on static load, drop height, and cushion thickness. Experimental data is often not available for all the range of environmental conditions. Further, use of maximum acceleration data for cushioning design is restricted to very simple cases. For example, they don't provide a means of calculating cushioning for drops with rotation. The effect of a drop impact upon a packaged product depends not only on the maximum deceleration, but also on the shape of the pulse. Hence, it is desirable to have more comprehensive information about the mechanical behaviour of foam during a load pulse.

There is a general understanding that compression properties of flexible foams are determined by buckling of the compressed cells filaments.[3–6] However, no time dependence of buckling has been considered, despite experimental evidence that this process is time-dependent.[6] Theoretical considerations also show that buckling in media subjected to relaxation is time-dependent,[7] and this should be taken into account.

It is desirable therefore to obtain stress–strain foam characteristics from high-speed impact experiments, in a view to providing an analytical approach to the design of cushioning. In Ref. 8 such an investigation was performed up to the speed of 5.5 m/s. However, the information obtained in this work is still not sufficient and needs to be completed.

This work is an attempt to provide a more comprehensive description of dynamic compression properties of flexible foams convenient for use in the conditions of short duration impacts, such as might result from mishandling of a cushioned product.

Journal of Applied Polymer Science, Vol. 30, 333–343 (1985)
 CCC 0021-8995/85/010333-11$04.00

MATERIALS

Basic experiments were performed with the polyether polyurethane foam A23-100, manufactured by Olympic Duoflex, which is commonly used in Australia as a cushioning material for packaging. This is a regular grade foam. Microscopic observations show that although essentially open-celled, this foam contains a considerable number of cell membranes. Because of this, qualitative results have been checked with a perfect polyester reticulated flexible foam Meracell 100 (Me 100) manufactured by Cable Makers Australia. Some numerical data on these foams is presented in Table I. Although the structure of both foams is isotropic within 10%, care was taken to load the foam A23-100 along the rise direction. Table I shows that the foam Me 100 is more uniform in cell sizes than A23-100.

Comparative tests have shown complete similarity of all the qualitative compression properties of the tested foams. We might conclude therefore that the membranes in A23-100 do not effect their mechanical properties and that pneumatic effects are absent, except perhaps at the very maximum speed of loading. This is in correspondence with Ref. 9, where it was estimated that the thickness of the membranes is some 100 times less than that of the filaments. Theoretical calculations of the pneumatic effect based on data[9] on the resistance of the polyurethane foam to the air flow also confirm this. Hence theoretical models of pneumatic damping, like Ref. 10, are not applicable in our case.

APPARATUS AND PROCEDURE

Static compression measurements were performed on the Lorentzen and Wettre CTT-300 Compression Tester. A speed of 0.2 mm/s was used.

Dynamic compression tests were conducted as free drops with the help of a single-arm drop tester (Fig. 1). To exclude preloading, the foam specimen (1) was fixed below a cradle (2) with soft PVC adhesive tape (3). The cradle with the specimen was dropped from the arm (4) of the tester. During the test the arm (4) is initially pulled downward, disconnecting from the cradle, and is then removed sideways to provide pure free fall conditions.

All measurements were performed at ambient temperature 20°C.

Samples of foam were cut to the dimensions 210 × 210 mm, with thickness of 105 and 50 mm used in different experiments. As a rule, for each measurement a fresh specimen was used which had not been previously subjected to any load. Exceptions to this only occured when investigating the effect of repeated loadings.

The readings of the accelerometer (5) were recorded on an FM tape recorder, Bruel and Kjaer type 7003, and then analyzed with the Hewlett-

TABLE I
Properties of the Tested Foams

	Density (kg/m^3)	Average cell size (mm)	Standard deviation of the cell size (mm)
A23-100	23	0.52	0.23
Me 100	28	0.52	0.16

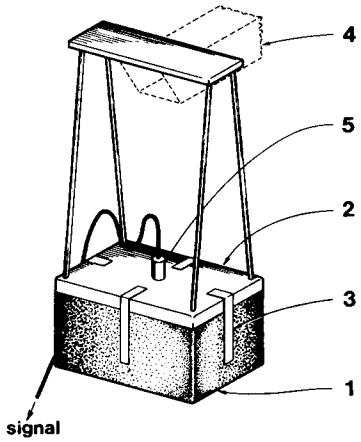

Fig. 1. Drop test apparatus: (1) foam specimen; (2) cradle of the prescribed weight; (3) adhesive tape; (4) arm of the drop tester; (5) accelerometer.

Packard Fourier Analyzer 5451B. The record was entered in the memory block of the analyzer using the maximum number of channels (in our case 2048). A typical record is presented in Figure 2. Operating with a large number of channels permitted us to see all of the drop process—flight, impact, and secondary rebounds—at the same time retaining all important details of the impact for subsequent investigation. The accelerometer readings always contain some parasitc DC component. Using the full picture of the drop process allowed us to eliminate this.

Curve B in Figure 2 presents the results of numerical integration—i.e., the velocity of the drop. For our analysis the first integration was used to obtain the specimen strain rate, and the second integration was performed to find strain.

Obvious calculations utilising the specimen dimensions and mass of the cradle yield compression stress from the deceleration of an impact.

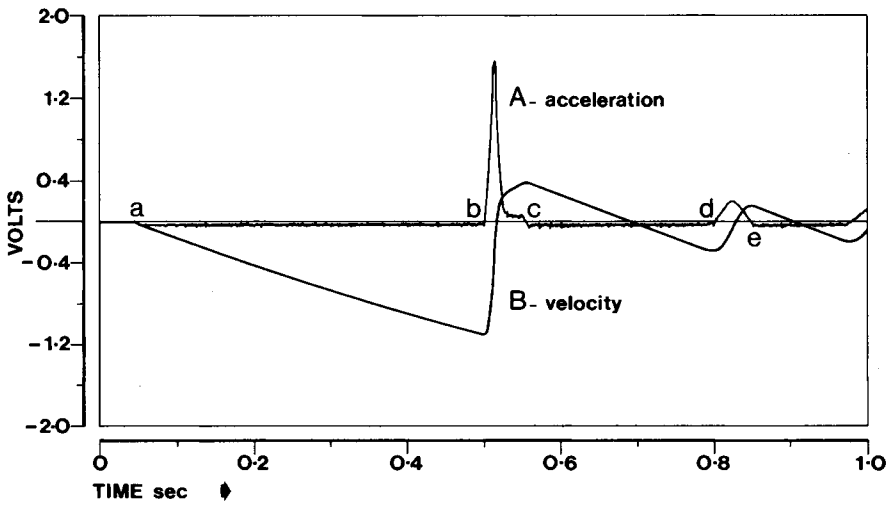

Fig. 2. Record of a typical drop test: (A) acceleration; (B) velocity; (a) start of a fall; (b, c) drop impact; (c, d) rebound flight; (d, e) first rebound impact.

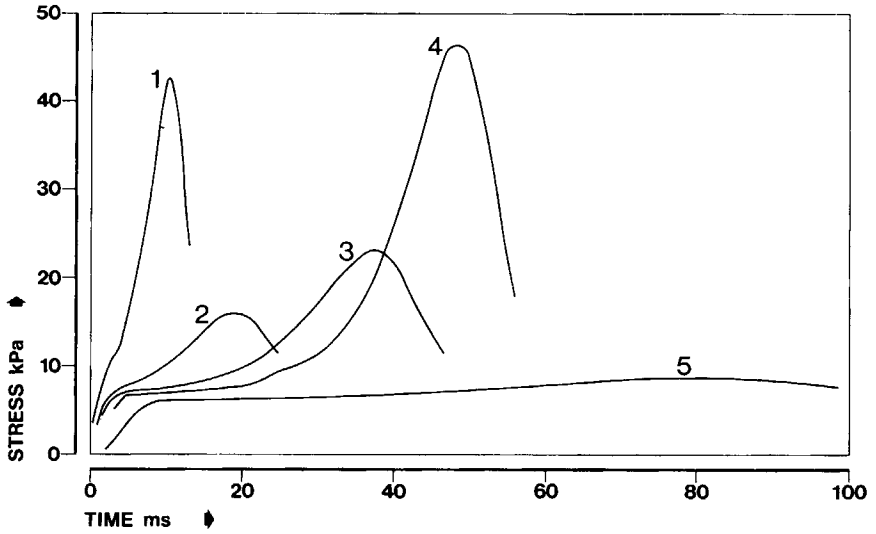

Fig. 3. Drop impacts for the tests of foam A23-100. Numeration of the curves is in accordance with specimen numbers (Table II).

EXPERIMENTAL RESULTS

Impact pulses for different combinations of loads and drop heights for the A23-100 foam are shown in Figure 3. Corresponding stress–strain curves and static stress–strain curve are presented in Figure 4. Here and below strain is defined as a ratio of the contraction of the foam during an impact to the initial thickness. The returning branches of the curves represent foam behavior during rebound, when deflection decreases.

Figure 4 shows that stress is greatly dependent on the rate of deformation. So the result of static measurements cannot be used for package design calculations, nor to judge efficiency E or ideality I of the foam in real conditions. The last parameters were introduced in Refs. 1 and 2 to estimate quality of a foam as a shock absorber and are defined with the equations

$$E = \frac{1}{\sigma_m} \int_0^{\epsilon_m} \sigma \, d\epsilon, \qquad I = E/\epsilon_m \tag{1}$$

where ϵ_m and σ_m are maximum strain and stress, correspondingly. Figures 5 and 6 show that both of these parameters are also strongly dependent on deformation rate.

Tests of both foams listed in Table I show that their static stress–strain dependence can be described with good accuracy with an equation of the form

$$\sigma = \alpha + \beta/(1 - \epsilon)^2 \tag{2}$$

where σ is stress, ϵ is strain, and α and β are empirical parameters. Of

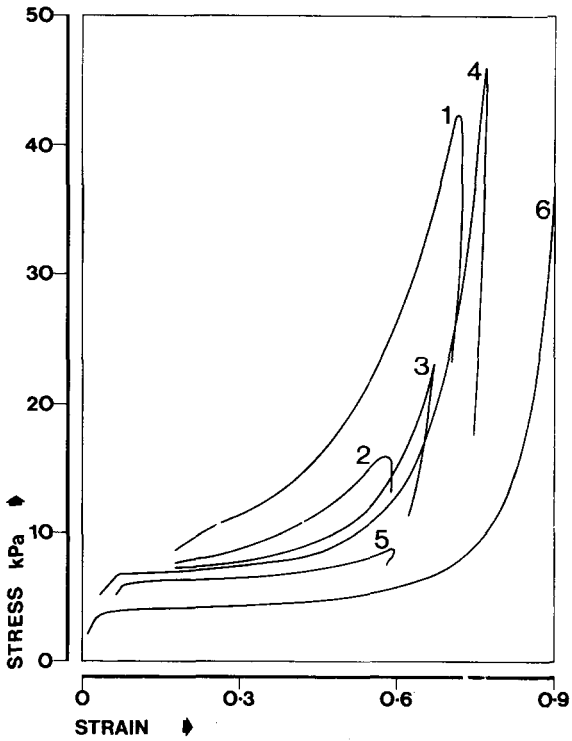

Fig. 4. Stress–strain curves for foam A23-100. (1–5) as in Figure 3; (6) static measurements.

course, this equation is not applicable to the range of small strains—less than about 0.05—where σ and ϵ reach zero simultaneously.

In the range of large deformations stress–strain dependence is strongly nonlinear. Because of this, the mathematical apparatus of linear viscoelasticity is not applicable. However, to procure an instrument for cushioning calculations, we have made an attempt to extrapolate eq. (2) to dynamic properties, with the assumption that the parameters α and β depend on the initial velocity of deformation, v. Actually, they would depend on the deformation rate during the entire impact, but as a first approximation, this hypothesis looks reasonable. Using the data of Figure 4, we find that for the A23-100 foam eq. (2) can be rewritten as

$$\sigma\ (\text{kPa}) = 3.6 + 1.5\,[1 - \exp(-0.7v)] + (0.34 + 0.03v)/(1 - \epsilon)^2 \qquad (3)$$

where v is expressed in s^{-1}. This formula was used to calculate the maximum strain and deceleration of the cushioned load in our drop tests, with the use of measured values of v. The results are presented in Table II. They show that calculations by the proposed formula (3) allow us to estimate the maximum deceleration with an accuracy of about 20% and the maximum strain with accuracy about 8%. This is sufficient for many practical purposes.

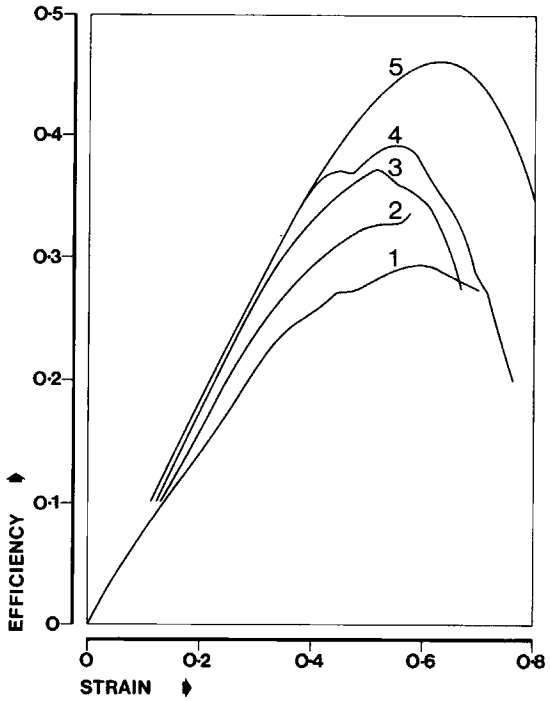

Fig. 5. Efficiency of foam A23-100. Curves 1–4 are numbered in accordance with Table II. Curve 5 is for static measurements.

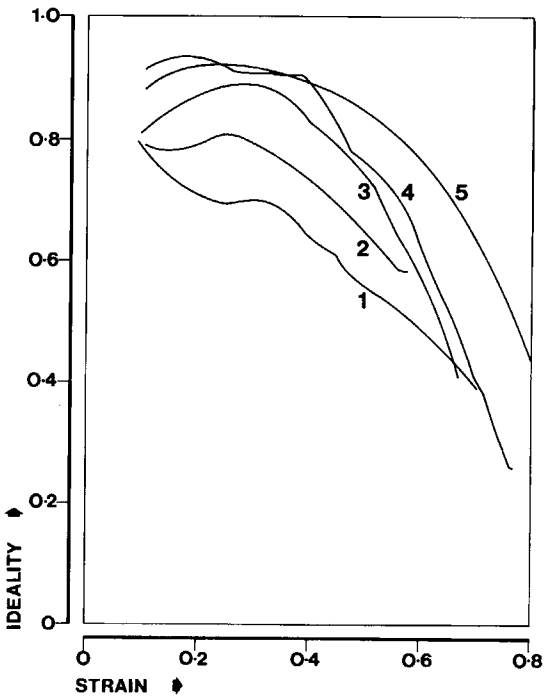

Fig. 6. Ideality of foam A23-100. Curves are numbered as in Figure 5.

TABLE II
Data for the Specimens of the Foam A23-100

Specimen no.	1	2	3	4	5
Specimen thickness (mm)	51.5	105	105	105	105
Load weight (kg)	2.3	2.3	6.7	12.6	12.6
Drop height (mm)	1500	1500	500	300	100
Measured initial speed of deformation (1/s)	96	46	27.1	22.1	12.1
Maximum deceleration (g)					
Measured	83	32	15.2	16.0	2.15
Calculated	100	32	12.9	14.5	2.27
Maximum strain					
Measured	0.72	0.59	0.69	0.77	0.61
Calculated	0.73	0.61	0.72	0.83	0.57

Formula (3) is convenient for the numerical calculation of the usual differential equations of dynamics. For a flat drop

$$h\sigma\, d\epsilon = mV\, dV, \quad h\, d\epsilon = V\, dt \tag{4}$$

where V is load velocity, m its mass per unit area, and h is foam thickness. The accepted simplifications imply that v is not variable during the integration of σ by ϵ. The use of eqs. (3) and (4) permits us to obtain not only the maximum values of acceleration and deflection, but also the shape of the impact pulse on the rise side. For rotational problems, the mechanical equations for rotational movement must be used instead of (4). Distribution of v along the radius of rotation would give the stress distribution with the help of eq. (3).

THEORETICAL CONSIDERATIONS

Previous theoretical studies based on microscopic observations[3-6] resulted in the general understanding that the mechanical behavior of a foam is governed by a buckling process. In view of this, it seems desirable to explain empirical eq. (2) from the buckling process point of view. This can be done by taking into consideration the highly nonuniform distribution of the cell sizes in even the most perfect flexible foam (see Table I). While the average cell sizes of the studied foams were about 0.5 mm, cell diameters from 0.2 to 1.0 mm were frequently encountered. Besides, small cells tend to have a greater probability of being closed with membranes than the large cells, thus forming rigid nuclei of material not subjected to local filament bending or buckling. On the other hand, the large cells tend to behave as stress concentrators in the medium, like holes in a strained strip of continuous matter. Our microscopic observations frequently show buckling threads at the edges of a large cell at the diameter across the direction of compression. Such buckling causes collapsing and folding of the large cells.

Thus, an estimation of the process of foam compression has been made with the following model. There are some rigid nuclei (small cells clusters) distributed in an averaged medium. Buckling would occur due to a local

stress concentration at filaments situated between rigid areas—otherwise no force great enough to cause buckling could be generated. In the process of deformation, bigger cells collapse, and rigid nuclei come closer together. Hence the number of filaments subjected to buckling increases. Let the relative number of filaments subjected to a buckling stress be N. Let this stress be greater than the average stress in the rest of the material by a factor k. Then the stress σ averaged through all the area including highly strained and moderately strained parts should be

$$\sigma = \sigma_c N + \frac{1}{k}\sigma_c(1 - N) = \frac{\sigma_c}{k} + \sigma_c N\left(1 - \frac{1}{k}\right) \tag{5}$$

where σ_c is a critical stress causing buckling. In this formula N is proportional to the probability of two rigid nuclei meeting each other, in other words, to the square of the density of the nuclei. During deformation bigger cells collapse, and the rigid nuclei come closer to each other; hence their density is proprotional to the ratio of initial volume of the foam to its deformed volume. As this ratio equals $1/(1 - \epsilon)$, and the term σ_c/k does not depend on strain ϵ, we arrive at formula (2).

We need also to take into account the fact that flexible foam is a viscoelastic material. This means filaments subjected to a stress close to σ_c are collapsing with time. This process has been considered in detail in Ref. 7. Here it is mentioned that N is strongly dependent on the velocity of deformation, v, because the faster the process the more highly stressed the filaments become before buckling. This gives a qualitative explanation to formula (3): N is effected primarily by velocity, with the first term depending only slightly on velocity. It is important to note, however, that in (3) the mathematical shape of this dependence must be considered as purely empirical.

The mechanism of filament buckling also explains some events related to the repeated loading of a foam specimen. When a specimen is loaded on a compression table to a significant strain and then released and loaded again immediately (Fig. 7), the stress–strain curve of the repeated loading (curve 2) will be significantly lower, apparently due to lower buckling stress σ_c. This could be expected, because the threads prebent in the first test would have less buckling resistance. After a while, their resistance is significantly, but not completely, recovered due to relaxation processes within the filaments (curve 3). Similar phenomena were observed in Ref. 11.

Further confirmation of this mechanism was obtained through repeated drops of foam specimens. Figure 8 shows two accelerometer records for successive drops of specimen 5 (Table II). During the second drop the record starts from a lower acceleration. Later the acceleration becomes much higher than with the first drop, because the strain of the foam increased. However, this effect is much milder than for the static loading case: The ratio of plateau stress levels in successive static loadings (Fig. 7) was 1.8 in comparison with 1.2 for the dynamic case (Fig. 8). In our experiments this effect was almost unnoticeable for the maximum deformation rates (sample 1). Such a dependence is of special importance to foams used in cushioning.

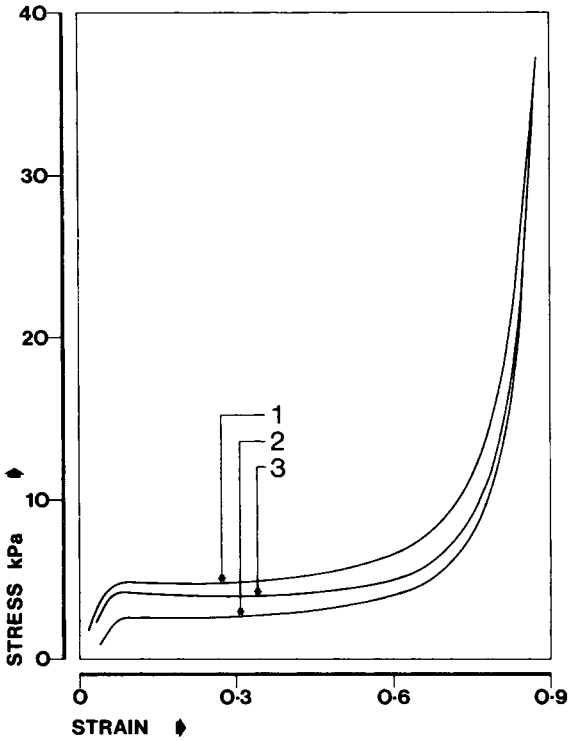

Fig. 7. Stress–strain curves for foam Me 100 in successive loadings. (1) first loading; (2) second loading, immediately following; (3) third loading, after 64 h.

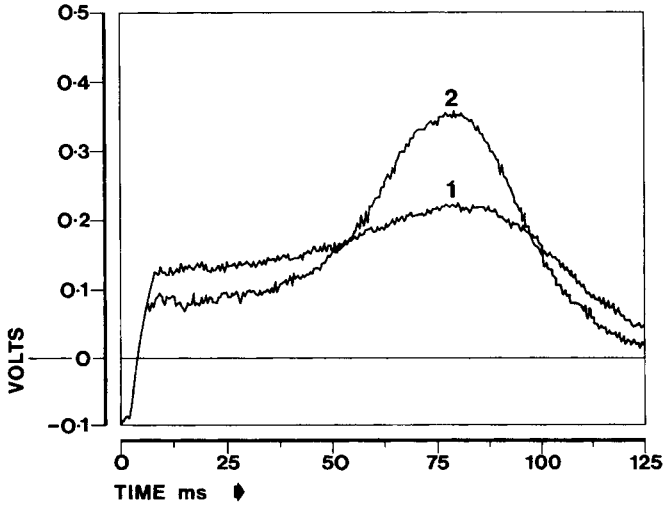

Fig. 8. Accelerometer records of two successive drops. Foam A23-100, specimen 5.

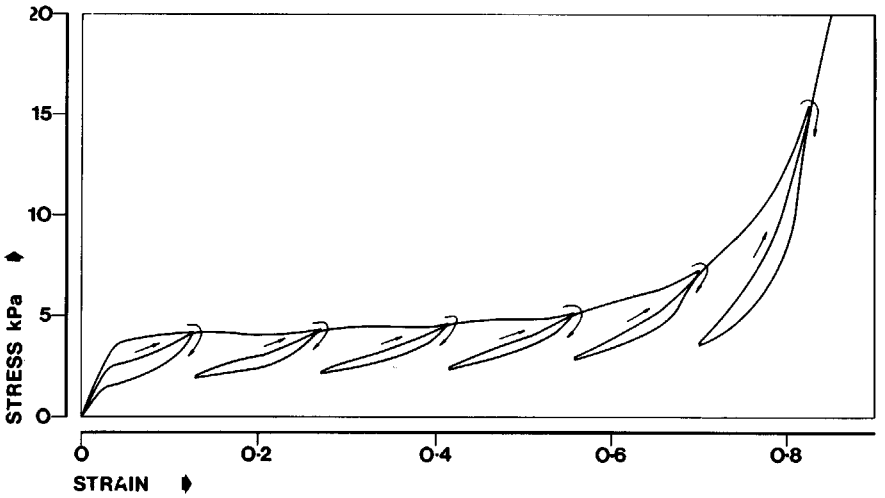

Fig. 9. Static loading of foam A23-100 in successive loops.

If after the first incidental impact the cushioning properties had deteriorated as severely as shown in Figure 7, this would have been quite impractical. Happily, with short durability impacts foams tend to retain their cushioning properties.

Physically this strain rate dependence is due to the inelastical nature of filament buckling. In short duration impacts, creep buckling is not a developed process, and elastic buckling mainly occurs. Hence, filaments that buckle elastically can almost fully recover after being released from their loaded state.

Interesting results are obtained in a static test with partial releasing of a sample during compression and then resuming the process of loading in successive loops (Fig. 9). After each loop the load comes back to the previous point of maximum deformation, and the stress–strain dependence returns to the initial loading curve. It is evident the loading curve does not depend on previous partial unloadings; further buckling involving new filaments.

The creep buckling model of compression properties, taking into account the nonuniform cell size distribution, can explain all the observed experimental results for open-celled foams: (1) exponent 2 in formulas (2) and (3); (2) strong strain rate dependence of the hyperbolic term in these formulas; (3) the decrease in foam resistance after the first compression and its partial recovering after some period of time; (4) mitigation of this effect for high strain rates; (5) return of the stress–strain dependence to the initial curve when loading in successive loops.

The cooperation of Olympic Duoflex and Cable Makers Australia is greatly appreciated. This work has been presented at the 14th Australian Polymer Symposium, February 12–16, 1984.

References

1. J. Miltz and G. Gruenbaum, *Polym. Eng. Sci.*, **21**(15), 1010 (1981).
2. G. Gruenbaum and J. Miltz, *J. Appl. Polym. Sci.*, **28**, 135 (1983).
3. A. N. Gent and A. G. Thomas, *J. Appl. Polym. Sci.*, **1**(1), 107 (1959).

4. A. N. Gent and A. G. Thomas, *Rubber Chem. Technol.*, **36**, 597 (1963).
5. R. E. Whittaker, *J. Appl. Polym. Sci.*, **15**, 1205 (1971).
6. G. A. Campbell, *J. Appl. Polym. Sci.*, **24**, 709 (1979).
7. V. O. Shestopal and P. C. Goss, *Acta Mechanica*, to appear.
8. J. W. Melvin and V. L. Roberts, *J. Cell. Plast.*, **7**, 97 (1971).
9. R. E. Jones and G. Fesman, *J. Cell. Plast.*, **1**(1), 200 (1965).
10. A. N. Gent and K. C. Rusch, *Rubber Chem. Technol.*, **39**(2), 389 (1966).
11. J. Miltz and G. Gruenbaum, *J. Cell. Plast.*, **17**(4), 213 (1981).

Received February 28, 1984
Accepted May 29, 1984